20th Annual Conference of the Canadian Nuclear Society
Montreal, Quebec, Canada / May 30 - June 2, 1999

COMPARISON OF MCNP4B AND WIMS-AECL CALCULATIONS OF COOLANT-VOID-REACTIVITY EFFECTS FOR UNIFORM LATTICES OF CANDU® FUEL

K.S. Kozier

Atomic Energy of Canada Limited
Chalk River Laboratories

SUMMARY

This paper compares the results of coolant-void reactivity (CVR) reactor-physics calculations performed using the Monte Carlo N-particle transport code, MCNP version 4B, with those obtained using Atomic Energy of Canada Limited's (AECL's) latest version of the Winfrith improved multigroup scheme (WIMS) code, WIMS-AECL version 2-5c. Cross sections derived from the evaluated nuclear data file version B-VI (ENDF/B-VI) are used for both the WIMS-AECL and MCNP4B calculations. The comparison is made for uniform lattices at room temperature containing either fresh natural uranium or mixed oxide (MOX) 37-element CANDU fuel. The MOX fuel composition corresponds roughly to that of irradiated CANDU fuel at a burnup of about 4500 MWd/tU. The level of agreement between the CVR predictions of WIMS-AECL and MCNP4B is studied as a function of lattice buckling (a measure of the curvature of the neutron-flux distribution) over the range from 0.0 to 4.1 m^{-2}. For the cases studied, it is found that the absolute k_{eff} values calculated by WIMS-AECL are higher than those of MCNP4B by several mk (1 mk is a change of 0.001 in k_{eff}), amounts that depend on the fuel type being modelled and the particular cross-section data used. However, the agreement between WIMS-AECL and MCNP4B is much better for the CVR (i.e., the Δk_{eff} on coolant voiding), and is relatively insensitive to the fuel type.

1. Introduction

Coolant-void reactivity (CVR) refers to the change in core reactivity that occurs when (heavy-water) coolant is removed from the fuel channels of CANDU power reactors. For current CANDU reactors using natural uranium fuel, the CVR is positive and is a key parameter in the analysis of design-basis accidents, such as large loss-of-coolant accidents (LOCAs), since it leads to an overpower transient.

The evolution of CVR-induced power transients is studied using three-dimensional, whole-core reactor models, using simplified reactor-physics information (homogenized, few-group cross sections and diffusion coefficients) for each lattice cell, derived from calculations using a lattice-cell code such as WIMS-AECL [1], which is AECL's version of the Winfrith improved multigroup scheme (WIMS [2]) code. The adoption of WIMS-AECL for general use in CANDU safety and licensing assessments requires its validation for reactor-physics phenomena that are important to safety. The primary validation is against measurements, such as measurements of critical lattice bucklings, but code-to-code benchmark comparisons with the results of CVR calculations using the Monte Carlo

N-particle (MCNP) transport code version 4B [3] provide a supplementary check and a means of extending the validation to conditions and quantities that are not practical to study by experiment.

WIMS-AECL is a deterministic code that solves the multigroup neutron-transport equation in two dimensions using collision-probability and other methods. For the zero-neutron-leakage case of an infinite lattice, it is straightforward to compare the CVR values calculated by WIMS-AECL with those determined by other codes. Several such comparisons have been made with the results of calculations using MCNP4B for a variety of assumed lattice conditions, with generally good results [4,5,6].

Neutron leakage, which can have a significant effect on the calculated CVR, is treated in WIMS-AECL by modifying the results of an infinite-lattice calculation according to the values provided for the radial- and axial-buckling parameters. For the uniform-lattice cases studied here, the radial or transverse buckling is zero. The axial-buckling values are determined from axial-flux profiles obtained from companion MCNP4B simulations for a range of lattice heights.

In the MCNP4B Monte Carlo transport calculations, the histories of individual neutrons are tracked using an explicit three-dimensional representation of the lattice and cross sections that are continuous functions of neutron energy. For the cases considered here, the material composition is homogeneous in the axial direction. Applying a vacuum-boundary condition to the flux at one axial end surface of the MCNP4B model allows some of the neutrons to escape, and the axial-flux profile assumes the shape corresponding to a bare, homogeneous slab reactor.

In the homogenized diffusion-theory approximation, the scalar flux solution for this simple lattice case is separable in space and energy, and the axial-flux profile, $\Phi(z)$, has a cosine shape:

$$\Phi(z) = \Phi_0 \cos(B_z z) \qquad (1)$$

Here, z is the axial distance from the lattice midpoint, Φ_0 is the flux at the midpoint and B_z^2 is the axial geometric buckling of the lattice. Only in the case of a critical lattice (k_{eff}=1) is this buckling equal to the material buckling of the lattice.

The numerical procedure of determining axial bucklings by fitting cosine functions to the axial-flux profiles is essentially the same as that used in experimental measurements of critical lattice bucklings, such as those performed in the ZED-2 (zero-energy deuterium) research reactor at the Chalk River Laboratories, where flux profiles are obtained from activation foils. Moreover, the technique of using MCNP to generate axial-flux profiles to determine bucklings and axial-diffusion coefficients has been thoroughly investigated by Milgram [7,8,9,10] in comparisons with the results of calculations using both WIMS-AECL and DRAGON [11]. The principal technical difference is that Milgram used a thick iron plug to terminate his MCNP lattice model to better simulate the neutron-leakage conditions at the end of a fuel channel in an operating CANDU power reactor. The present work emphasises code-to-code comparison with WIMS-AECL results for fresh natural uranium (FNU) and MOX fuel

at room-temperature conditions, and is more directly relevant to the ZED-2 critical-buckling measurements.

During the course of this work, new versions of the WIMS-AECL code and its evaluated nuclear data file version B-VI (ENDF/B-VI)-based cross-section data library became available. The impact of these new versions on the comparison with MCNP4B is examined along with certain WIMS-AECL case-modelling options.

2. Method

2.1 MCNP4B Calculations

Sixteen MCNP4B models were constructed to represent the square, 28.575-cm-pitch, 37-element CANDU fuel lattice cell shown in Figure 1 for cooled or voided, FNU and MOX fuel at three different axial lattice heights (362.23 cm, 262.54 cm and 150.00 cm), plus the fully reflected case. The specific values of 362.23 cm and 262.54 cm were chosen because the cooled and voided MOX fuel lattices are very near criticality at these values, respectively (see Table 1); hence, the total neutron-leakage and -flux spectral characteristics for these cases will be similar to those obtained with this fuel in critical lattice experiments. The total geometric buckling of an operating CANDU power reactor is similar to the axial-buckling values obtained at the lattice height of 362.23 cm (~0.7 m^{-2}). The cases with a lattice height of 150.00 cm have an axial buckling of about 4.1 m^{-2}, a value that is roughly comparable to the total geometric buckling of a typical ZED-2 lattice configuration.

Taking advantage of symmetry, only a one-quarter segment of the lattice cell of half the full lattice height is modelled explicitly. A (specular, or mirror-like) reflective-boundary condition is used at all cell-boundary surfaces except for the finite cases, which have a vacuum-boundary condition at one axial end, created by adding an adjoining cell with zero neutronic importance.

The terms “cooled” and “voided” refer to the presence or absence of heavy-water coolant inside the pressure-tube region shown in Figure 1. In both the MCNP4B and WIMS-AECL cases, the voided state is represented by reducing the coolant density by a factor of 10 000. The coolant and moderator are modelled with the same composition, corresponding to an isotopic purity of 99.65 wt% D_2O.

The only changes to the model between the FNU and MOX cases are the fuel composition and density. The MOX fuel composition includes uranium depleted to 0.37 wt% ^{235}U in U, 0.3 wt% Pu and 0.05 wt% Dy, the latter to simulate fission products. This combination roughly approximates the basic neutronic characteristics (e.g., material buckling) of typical irradiated CANDU fuel at a burnup of about 4500 MWd/tU.

The MCNP4B model differs slightly from an actual CANDU fuel bundle in that bundle end-region details, fuel-pellet details and element appendages are ignored. However, this is not important for a code-to-code comparison.

The detailed input files for the finite cases are very similar to those reported in Reference 4 for an infinite lattice cell, but with axial-plane surfaces added for determining surface-flux tallies. For the shortest model these surfaces are spaced every 2.5 cm, while the two larger lattices use planes spaced 5.0 cm apart.

Care was taken to build up a converged neutron-source distribution for each case individually in eight steps prior to the final MCNP4B run. Typically, this involved starting with 19 source neutrons distributed explicitly along the fuel channel and running 110 cycles (skipping the first 10 cycles) with 100 source neutrons for the initial case. The number of source particles was increased in steps until it reached 20 000 (50 000 in a few cases). The final MCNP4B cases used this converged starting neutron-source distribution with at least 4.0×10^7 active neutron histories (up to 6.0×10^7 in a few cases). This large number of histories is necessary to achieve an acceptable accuracy of roughly ±1% for the fitted geometric bucklings.

The k_{eff} values reported in Table 1 are the final combined collision/absorption/track-length k_{eff} values with one-sigma uncertainties. The surface neutron-flux tallies were performed in four neutron-energy groups: thermal (0.0 eV to 0.6 eV), epithermal (0.6 eV to 100 eV), resonance (100 eV to 0.1 MeV) and fast (0.1 MeV to 20 MeV).

2.2 Axial Geometric Buckling Determinations

The geometric buckling values were determined by fitting Equation (1) to the axial flux profiles obtained from the MCNP4B surface-flux tallies. The fitted bucklings are based on the total flux (i.e., the sum over all energies) averaged across the lattice cell, as this provides the best statistics and is consistent with the assumption that the buckling is independent of neutron energy. The spatial region in which this assumption (and hence diffusion theory) is valid was tested by examining the variation in the spectrum index, defined in a two-group treatment as the ratio of the thermal flux to the fast flux [12].

The spectrum index was calculated as a function of axial position with the flux data above 0.6 eV combined into a single fast energy group. An asymptotic value for the spectrum index at the midpoint of the lattice was determined by averaging the values for all positions at distances ≥50 cm removed from the vacuum boundary (see Table 1). It was observed that the spectrum index converged to within about ±0.1% of its asymptotic value at a distance of about 30 cm inside the vacuum boundary in most cases. Accordingly, only the flux-tally data at distances ≥30 cm removed from the vacuum boundary were used in the buckling determinations. However, selecting a fixed data cutoff distance at 30 cm is a compromise that has a small impact on the buckling values determined, since they depend somewhat on which data points are included in the fit.

2.3 WIMS-AECL Calculations

WIMS-AECL calculations were performed at the axial geometric buckling values determined from the MCNP calculations. Five sets of k_{eff} values are compared in Table 2, corresponding to the following options:

1. **WIMS-AECL reference model**. This case corresponds to the standard WIMS-AECL model typically used for routine production-type calculations for CANDU reactors with the recommended options to obtain adequate precision at optimum computational efficiency. For example, it uses a specific set of 33 neutron-energy groups in the transport calculations, and employs the P_{ij} collision-probability method within a radial distance of 7.8 cm from the centre of the lattice cell and the Perseus method for the balance of the cell. The main change in version 2-5c of the WIMS-AECL code is a new collision-probability routine that corrects deficiencies in the axial-diffusion-coefficient calculations for optically thin regions, which were identified by Milgram [13,14] in earlier comparisons with MCNP results. The reference model uses the new collision-probability treatment for the diffusion-coefficient calculation, but not for other aspects of the calculation. The main improvement in the new ENDF/B-VI-based WIMS-AECL data library (file named 1998 July 29, u2x.1-0d.hpux10, ShZr, u238ren, u235r4) is the inclusion of resonance-shielded cross sections for Zr nuclides with separate data sets for the pressure tube, calandria tube and fuel cladding. The reference model also uses the recommended "U238" cross-section data, which incorporate an adjustment to maintain consistency with the way the ^{238}U data are processed in the earlier ENDF/B-V version of the WMS-AECL data library.
2. **Old diffusion-coefficient calculation**. This case corresponds to the reference case, but reverts to the old collision-probability treatment for the calculation of the diffusion coefficients.
3. **Unshielded Zr**. This case corresponds to the reference model, but uses the unshielded Zr cross sections that are available as an option in the new data library.
4. **U238NF**. This case corresponds to the reference model, but uses the unadjusted "U238NF" data for ^{238}U, instead of the recommended "U238" data.
5. **"Best estimate" model**. This case removes many of the simplifications in the reference model that accelerate its execution. In particular, the "best estimate" model uses:
    - all 89 neutron-energy groups,
    - the P_{ij} collision-probability solution technique for the full problem geometry, together with more numerous annuli defined in the coolant and moderator regions, and
    - the new collision-probability method in the resonance and neutron-flux calculations in cylindrical geometry, as well as in the diffusion-coefficient calculations.

The detailed WIMS-AECL case input files used in this study are similar to those listed in Reference 4.

3. Results

3.1 MCNP4B Results

The key reactor-physics results from the MCNP4B calculations are listed in Table 1. Included is a direct measure of neutron leakage obtained from outward neutron current (i.e., direction cosine >0) tallies at the lattice vacuum boundary. This quantity is the leakage probability per source particle and is the same as the "weight loss to escape" printed in the MCNP4B problem summary table. Comparing the leakage probabilities for the cooled and voided states shows that neutron leakage increases by about 9% on coolant voiding.

The B_z^2 and asymptotic spectrum index values listed in Table 1 were determined as described in Section 2.2. The axial-buckling values for each lattice height are similar and show a small decrease on coolant voiding; this result is consistent with the observed increase in neutron leakage, which causes a slight increase in the extrapolated lattice height.

The asymptotic spectrum index values decrease (spectrum hardening) by about 10% over the range of bucklings studied for a given fuel and coolant state. At a fixed lattice height, the increase in neutron leakage and the loss of heavy water from the lattice cell on coolant voiding cause a similar decrease of about 10% in the spectrum index. In addition, the increase in absorption in going from FNU to MOX fuel causes roughly a 10% hardening of the spectrum.

Because the voided buckling differs slightly from the cooled value at the same lattice height, the voided k_{eff} values are adjusted to the cooled buckling values before the Δk_{eff}-on-coolant-voiding values are calculated. The corrections applied to the voided k_{eff} values were determined by fitting the data to the criticality equation of Fermi age theory:

$$k_{eff} = \frac{k_{\infty} e^{-B^2\tau}}{1 + B^2 L^2} \qquad (2)$$

where L^2 is the thermal-diffusion area and τ is the Fermi age (slowing-down area), although linear interpolation gives similar results.

The uncertainties listed for the Δk_{eff}-on-coolant-voiding values in Table 1 are based on the one-sigma uncertainties of the cooled and voided k_{eff} values. The true uncertainties will be larger, given the uncertainty in the buckling determination and the need for interpolation.

3.2 WIMS-AECL Results

The WIMS-AECL k_{eff} values for the different cases studied are listed in Table 2 at the same axial bucklings determined from the MCNP cases. These results are compared relative to the reference-model results before the latter are compared with the MCNP values. The differences in the

corresponding Δk_{eff}-on-coolant-voiding values relative to the reference-model results are shown in Figures 2a and 2b for the FNU and MOX fuel, respectively.

In every case in Table 2, the WIMS-AECL reference model produces the highest k_{eff} values. Reverting to the old collision-probability treatment for the diffusion-coefficient calculation produces only a slight difference in the cooled k_{eff} values, but gives a significant deviation that grows linearly with buckling for the voided cases. This leads to a linear dependence of the Δk_{eff} on coolant voiding with buckling, particularly for the FNU fuel, as shown in Figure 2a.

The cases using unshielded Zr cross sections have lower k_{eff} values by 1.8 to 2.9 mk, amounts that depend slightly on the lattice buckling, coolant state and fuel type. However, the net effect on the Δk_{eff} on coolant voiding is a minor upward shift of 0.1 to 0.3 mk that is relatively insensitive to lattice buckling, as shown in Figures 2a and 2b.

Using the unadjusted U238NF data decreases all the k_{eff} values by 2.2 to 3.2 mk, in a manner similar to the change induced by the unshielded Zr cross sections. However, the net effect on the Δk_{eff} on coolant voiding is a larger, constant increase of about 0.6 mk.

Finally, the "best estimate" WIMS-AECL model results show generally good agreement with the reference-model results, with k_{eff} values that are slightly lower by 0.6 to 1.1 mk. The net effect on the Δk_{eff} on coolant voiding is a small increase of 0.1 to 0.2 mk.

3.3 Comparison Between MCNP4B and WIMS-AECL Reference Model Results

The k_{eff} values obtained using the WIMS-AECL reference model are compared with the MCNP4B values in Figure 3. The WIMS-AECL values for FNU fuel are seen to be higher than the MCNP4B values by 7.4 to 8.7 mk, while the MOX values are higher than the MCNP4B values by 4.6 to 5.8 mk. For both fuel types, the results show similar behaviour on coolant voiding, and increase slightly with lattice buckling.

The corresponding values for the Δk_{eff} on coolant voiding are compared in Figure 4. It is seen that the Δk_{eff}-on-coolant-voiding values obtained using the WIMS-AECL reference model are slightly lower than the MCNP values for both FNU and MOX fuel by a similar amount. The average difference is -0.17 mk, indicated by the solid horizontal straight line in Figure 4. Uncertainty bands at the $\pm 2\sigma$ level based on the precision of the MCNP calculations are shown as dashed lines.

4. Discussion

The absolute k_{eff} values for the WIMS-AECL reference case are higher than the MCNP4B values by several mk, amounts that are somewhat larger than reported in similar comparisons between MCNP4B and HELIOS [15] calculations for infinite lattices [16]. Nevertheless, the HELIOS k_{∞}

values at 4000 MWd/tU reported in Reference 16 are closer to the MCNP4B values than are the values for FNU, as is the case for the WIMS-AECL MOX k_{eff} values in this work. Comparisons of HELIOS k_{∞} values with MCNP4B values for DUPIC fuel in Reference 6 show a similar trend.

The level of agreement between the WIMS-AECL and MCNP values for the Δk_{eff} on coolant voiding shows little difference between the FNU and MOX cases. This finding differs somewhat from the HELIOS results reported in Reference 16 for infinite lattices at the hot operating condition, which agree with MCNP4B for FNU, are higher by 0.3 mk at 4000 MWd/tU and lower by 1.1 mk at 13 000 MWd/tU. Additional room-temperature cases with a MOX fuel composition representative of a higher fuel burnup would be needed to confirm this trend.

The new collision-probability treatment implemented in WIMS-AECL version 2-5c improves the agreement between WIMS-AECL and MCNP4B for the Δk_{eff}-on-coolant-voiding values, eliminating a significant dependence on lattice buckling. This result confirms the findings of Milgram [14]. The magnitude of the correction involved appears to be greater for FNU fuel than for MOX.

The new resonance-shielded Zr cross sections in the WIMS-AECL ENDF/B-VI data library increase the absolute k_{eff} values by a few mk, as expected, and reduce the calculated Δk_{eff} on coolant voiding by a minor amount. This reduction is slightly greater for FNU than for MOX, by about 0.1 mk.

The adjusted U238 cross-section data in the WIMS-AECL ENDF/B-VI data library give better agreement with the MCNP4B Δk_{eff}-on-coolant-voiding values than do the unadjusted U238NF data, by about 0.4 mk for both FNU and MOX.

The "best estimate" WIMS-AECL case improves the agreement with the MCNP4B Δk_{eff}-on-coolant-voiding values for both FNU and MOX by a very small amount, about 0.15 mk. However, execution times for this case are about nine times greater than those for the WIMS-AECL reference model.

5. Conclusions

The k_{eff} values and the Δk_{eff} on coolant voiding calculated by WIMS-AECL and MCNP4B were compared for uniform lattices of FNU and MOX fuel at room temperature as a function of lattice axial buckling over the range from 0.0 to 4.1 m^{-2}. The main conclusions are:

1. While the WIMS-AECL absolute k_{eff} values are observed to be higher than the MCNP4B values by several mk and by amounts that differ significantly for the two fuel types studied, very similar results are obtained for the Δk_{eff} on coolant voiding. This finding indicates that the systematic offsets are largely cancelled out in the subtraction. Hence, at least at room temperature, the level of agreement between the two codes for the Δk_{eff} on coolant voiding is relatively insensitive to changes in the fuel composition, such as the isotopic transformations associated with fuel burnup.

2. When the new collision-probability treatment is used with WIMS-AECL version 2-5c, very little dependence on lattice buckling is observed for the comparison of the Δk_{eff} on coolant voiding, despite the significant change in the spectrum index that is associated with neutron leakage. This result confirms the findings of Milgram [14], and supports the view that CVR validation experiments performed in a high-geometric-buckling lattice such as ZED-2 are equally relevant to the low-geometric-buckling CANDU power-reactor circumstance.
3. The current set of recommended WIMS-AECL modelling options and cross-section data that define the "reference" case is confirmed as a computationally efficient choice that replicates the Δk_{eff} on coolant voiding calculated by MCNP4B to within about 0.2 mk for the idealized cases studied.

References

1. J.V. Donnelly, "WIMS-CRNL: A User's Manual for the Chalk River Version of WIMS", AECL Report, AECL-8955, 1986 January.
2. J.R. Askew, F.J. Fayers and P.B. Kemshell, "A General Description of the Lattice Code WIMS", Journal of the British Nuclear Engineering Society, 5:564-585, 1966.
3. J.F. Briesmeister, Editor, "MCNP - A General Monte Carlo N-Particle Transport Code, Version 4B", Los Alamos National Laboratory report LA-12625-M, Version 4B, UC 705 and UC 700, issued 1997 March.
4. A. Lone, "MCNP4B and WIMS-AECL Comparison of Coolant Void Reactivity Predictions of CANDU Fuel Infinite Lattices at Room Temperature", RC-2076, unpublished report, available from Chalk River Laboratories, Chalk River, Ontario, K0J 1J0, 1998 June.
5. M.S. Milgram, "Void Reactivity Predictions for an Infinite Lattice of 37-Element CANDU Fuel", Fourth Canadian Nuclear Society International Conference on Simulation Methods in Nuclear Engineering, Montreal, 1993 June 2-4.
6. H. Choi and A.A. Ferri, "A HELIOS Working Library for DUPIC Fuel", Proc. Int. Conf. on the Physics of Reactors (PHYSOR 96), Breakthrough of Nuclear Energy by Reactor Physics, Mito, Ibaraki, Japan, 1996 Sept. 16-20, Vol. 3, F-58, American Nuclear Society, 1996.
7. M.S. Milgram, "Estimates of Void Reactivity Coefficients with MCNP and WIMS-AECL", Proceedings of the Canadian Nuclear Society's 1994 Nuclear Simulation Symposium, Pembroke, 1994 Oct. 12-14, p.55-60.
8. M.S. Milgram, "Determination of Axial Diffusion Coefficients by the Monte-Carlo Method", presented at Int. Conf. Reactor Physics and Reactor Computation, Tel Aviv, Israel, 1994.
9. G. Marleau and M.S. Milgram, "A DRAGON-MCNP Comparison of Axial Diffusion Subcoefficients", Trans. Am. Nucl. Soc., Vol. 72, Philadelphia, 1995 June, p.163-4.
10. G. Marleau and M.S. Milgram, "A DRAGON-MCNP Comparison of Void Reactivity Calculations", 16th Annual Conf. Canadian Nuclear Society, Saskatoon, Saskatchewan, 1994 June 4-7.
11. G. Marleau, A. Hébert and R. Roy, "New Computational Methods Used in the Lattice Code DRAGON", Proc. Int. Topl. Mtg. Advances in Reactor Physics, Charleston, South Carolina, 1992 Mar. 8-11.

12. R.J.J. Stamm'ler and M.J. Abbate, "Methods of Steady-State Reactor Physics in Nuclear Design", Academic Press, 1983, p. 351.
13. M.S. Milgram, "Diffusion Coefficient for a Voided Annulus: The Trouble with COPRAN 1. The Self-collision Probability", Proceedings of the Joint International Conference on Mathematical Methods and Supercomputing for Nuclear Applications, Saratoga Springs, 1997.
14. M.S. Milgram, "Diffusion Coefficients and Collision Probabilities for Annular Regions of Low Optical Thickness II: The General Case", Annals of Nuclear Energy, Vol.26, No.10, 1999 Mar.
15. E.A. Villarino, R.J.J. Stamm'ler, A.A. Ferri and J.J. Casal, "HELIOS: Angularly Dependent Collision Probabilities", Nucl. Sci. & Eng., 112, 16, 1992.
16. F. Rahnema, S. Mosher, M. Pitts, S. McKinley, P. Akhtar, D. Serghiuta and R.J.J. Stamm'ler, "Void Reactivity Calculations in a Typical CANDU Cell Using MCNP and HELIOS", Proceedings of the International Conference on Physics of Nuclear Science and Technology, Long Island, N.Y., 1998 Oct.

Table 1. MCNP4B results

Fuel type	Coolant state	Lattice height (cm)	Fitted axial geometric buckling (m^{-2})	*k*-effective	Leakage probability per source particle	Asymptotic spectrum index	Δk_{eff} on coolant voiding (mk)
FNU	voided	infinite	0	1.14317 ± 0.00006	0	2.124	
		362.23	0.7285	1.11298 ± 0.00006	0.02510	2.083	
		262.54	1.3766	1.08745 ± 0.00007	0.04644	2.048	
		150.00	4.0953	0.98872 ± 0.00009	0.12934	1.907	
	cooled	infinite	0	1.11909 ± 0.00006	0	2.352	24.08 ± 0.08
		362.23	0.7345	1.09176 ± 0.00006	0.02291	2.307	20.98 ± 0.08
		262.54	1.3788	1.06827 ± 0.00007	0.04267	2.267	19.09 ± 0.10
		150.00	4.1165	0.97721 ± 0.00008	0.11921	2.111	10.80 ± 0.12
MOX	voided	infinite	0	1.04737 ± 0.00007	0	1.901	
		362.23	0.7288	1.02174 ± 0.00007	0.02346	1.866	
		262.54	1.3714	1.00004 ± 0.00008	0.04349	1.836	
		150.00	4.0805	0.91527 ± 0.00008	0.12150	1.717	
	cooled	infinite	0	1.02335 ± 0.00007	0	2.117	24.02 ± 0.10
		362.23	0.7362	1.00017 ± 0.00006	0.02141	2.077	21.32 ± 0.09
		262.54	1.3792	0.97996 ± 0.00008	0.04002	2.043	19.82 ± 0.11
		150.00	4.1237	0.90146 ± 0.00009	0.11228	1.910	12.54 ± 0.12

Table 2. Comparison of various WIMS-AECL calculation options

Fuel type	Coolant state	Axial buckling (m^{-2})	*k*-effective				
			reference model	old diffusion-coefficient calculation	unshielded Zr	U238NF	"best estimate" model
FNU	voided	0	1.15053	1.15053	1.14797	1.14792	1.14995
		0.7285	1.12085	1.12035	1.11844	1.11831	1.12022
		1.3766	1.09535	1.09444	1.09307	1.09288	1.09466
		4.0953	0.99692	0.99454	0.99514	0.99472	0.99603
	cooled	0	1.12672	1.12672	1.12393	1.12350	1.12606
		0.7345	1.09954	1.09950	1.09688	1.09640	1.09881
		1.3788	1.07646	1.07638	1.07393	1.07340	1.07567
		4.1165	0.98591	0.98572	0.98381	0.98313	0.98486
MOX	voided	0	1.05192	1.05192	1.04918	1.04955	1.05146
		0.7288	1.02664	1.02643	1.02404	1.02434	1.02615
		1.3714	1.00507	1.00469	1.00257	1.00283	1.00454
		4.0805	0.92088	0.91990	0.91879	0.91886	0.92023
	cooled	0	1.02813	1.02813	1.02528	1.02522	1.02756
		0.7362	1.00488	1.00484	1.00216	1.00204	1.00425
		1.3792	0.98520	0.98513	0.98256	0.98241	0.98453
		4.1237	0.90722	0.90704	0.90495	0.90466	0.90636

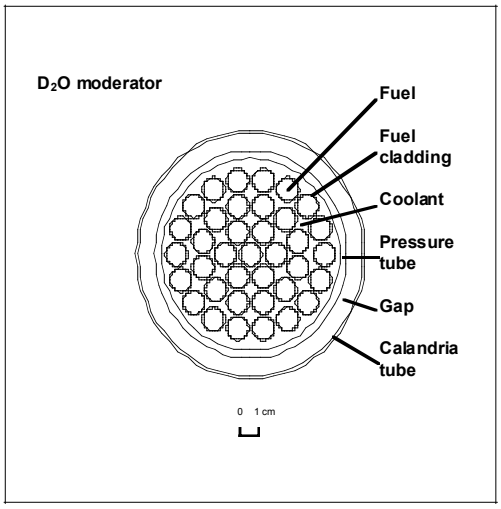

Figure 1. Cross section of a 37-element CANDU fuel lattice cell

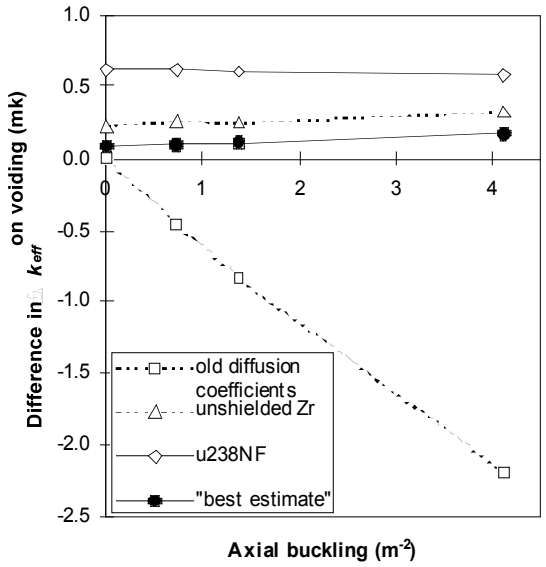

Figure 2a. Difference in WIMS-AECL Δk_{eff} on coolant voiding relative to reference model: FNU

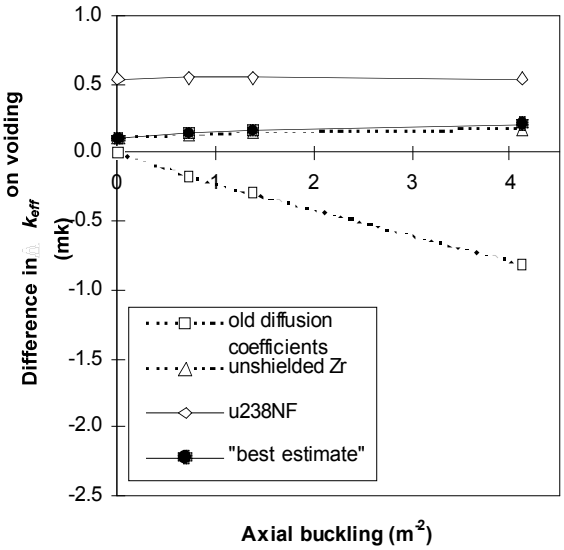

Figure 2b. Difference in WIMS-AECL Δk_{eff} on coolant voiding relative to reference model: MOX

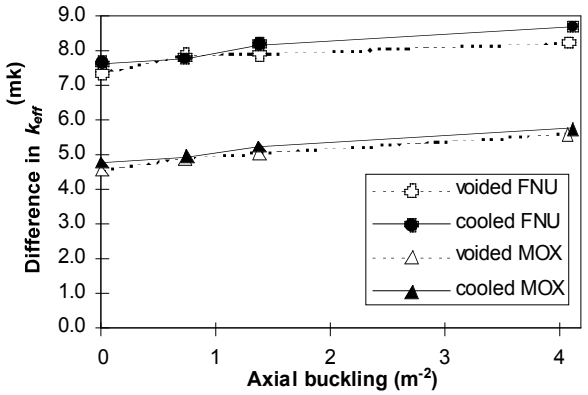

Figure 3. Comparison of k_{eff} values: WIMS-AECL reference minus MCNP4B

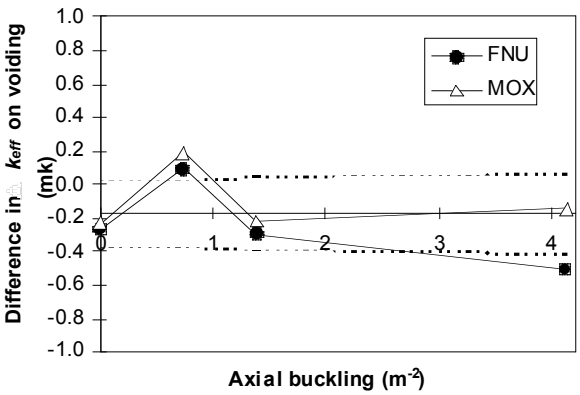

Figure 4. Comparison of Δk_{eff} on coolant voiding: WIMS-AECL reference minus MCNP4B